Available online at www.sciencedirect.com

SCIENCE DIRECT

Developmental Biology 281 (2005) 78 – 90

DEVELOPMENTAL BIOLOGY

www.elsevier.com/locate/ydbio

Secondary heart field contributes myocardium and smooth muscle to the arterial pole of the developing heart

Karen L. Waldo[a], Mary R. Hutson[a], Cary C. Ward[b], Marzena Zdanowicz[a], Harriett A. Stadt[a], Donna Kumiski[c], Radwan Abu-Issa[a], Margaret L. Kirby[a,*]

[a]*Neonatal-Perinatal Research Institute, Department of Pediatrics (Neonatology), Duke University Medical Center, Bell Building, Room 157, Box 3179, Durham, NC 27710, USA*

[b]*Department of Medicine (Cardiology), Duke University Medical Center, Durham, NC 27710, USA*

[c]*Department of Cellular Biology and Anatomy, Medical College of Georgia, Augusta, GA 30912, USA*

Received for publication 19 January 2005, revised 19 January 2005, accepted 10 February 2005
Available online 11 March 2005

Abstract

The arterial pole of the heart is the region where the ventricular myocardium continues as the vascular smooth muscle tunics of the aorta and pulmonary trunk. It has been shown that the arterial pole myocardium derives from the secondary heart field and the smooth muscle tunic of the aorta and pulmonary trunk derives from neural crest. However, this neural crest-derived smooth muscle does not extend to the arterial pole myocardium leaving a region at the base of the aorta and pulmonary trunk that is invested by vascular smooth muscle of unknown origin. Using tissue marking and vascular smooth muscle markers, we show that the secondary heart field, in addition to providing myocardium to the cardiac outflow tract, also generates prospective smooth muscle that forms the proximal walls of the aorta and pulmonary trunk. As a result, there are two seams in the arterial pole: first, the myocardial junction with secondary heart field-derived smooth muscle; second, the secondary heart field-derived smooth muscle with the neural crest-derived smooth muscle. Both of these seams are points where aortic dissection frequently occurs in Marfan's and other syndromes.

Keywords: Heart development; Outflow tract; Arterial pole; Myocardium; Smooth muscle; Cardiac neural crest; Secondary heart field

Introduction

The truncus of the outflow tract of the embryonic heart is added from a field of splanchnic mesoderm beneath the floor of the foregut called secondary heart field (Waldo et al., 2001). This field of cells is different from, or a subpopulation of, the anterior heart field described by two other laboratories (Kelly et al., 2001; Mjaatvedt et al., 2001). The differences in these fields have been discussed in a recent review (Abu-Issa et al., 2004). Cells in the secondary heart field express Nkx2.5 and Gata4, as do the cells of the primary heart fields (Waldo et al., 2001). Induction of myocardium from the secondary heart field progresses in a caudal direction as the outflow tract translocates caudally relative to the pharyngeal arches. As the cells in the secondary heart field begin to move into and differentiate as outflow myocardium, they initiate expression of HNK1, a marker of migrating cells, and then MF20, a marker of cardiomyocyte differentiation (Waldo et al., 2001). FGF8 and BMP2 are thought to induce the myocardial potential of the cells in a manner that mimics induction of the myocardium from the primary heart fields (Lough and Sugi, 2000; Waldo et al., 2001).

Even though the discovery of the secondary heart field sheds light on the origin of the distal outflow myocardium, no attention has been given to the origin of the vascular smooth muscle at the base of the aorta and pulmonary trunk. Cardiac neural crest-derived ectomesenchyme forms the vascular smooth muscle tunics of the aortic arch arteries (Le Lièvre and Le Douarin, 1975), but the neural crest-derived smooth muscle does not extend to the base of the pulmonary

* Corresponding author. Fax: +1 919 668 1599.
E-mail address: mlkirby@duke.edu (M.L. Kirby).

0012-1606/$ - see front matter © 2005 Elsevier Inc. All rights reserved.
doi:10.1016/j.ydbio.2005.02.012

trunk and aorta (Waldo et al., 1994). Two different models attempt to explain how the single lumen of the embryonic outflow tract becomes divided into the aortic and pulmonary channels (reviewed in detail by Thompson and Fitzharris, 1985). Briefly, the classical model describes the cranial-to-caudal formation of a divided lumen by the fusion of a longitudinal pair of spiraling endocardial cushions along the length of the common outflow tract lumen. Cranially, the fusing endocardial cushions are joined by the condensed mesenchyme of the aorticopulmonary septum that enters the dorsal aortic sac from the area between the fourth and sixth pairs of arch arteries and grows into the truncus arteriosus to divide the lumen into systemic and pulmonary channels. By the time the endocardial cushions have fused in the proximal outflow tract (conus), the aorta and pulmonary trunk and their semilunar valves have already been formed from the tissue distal to the fusing conal cushions suggesting that the truncal myocardium and endocardial cushions have become transformed into arterial smooth muscle and connective tissue (Arguello et al., 1978; Kramer, 1942; Patten, 1953). An alternative to the classical model rejects the idea that the distal truncus is reorganized into smooth muscle (Thompson and Fitzharris, 1979, 1985). Instead, the truncus rotates and retracts toward the ventricles. This is accomplished by a septation complex consisting of the distal myocardial rim of the truncus, the aorticopulmonary septum, and the adjacent bifurcation of the vascular lumen. The single outflow lumen becomes divided into two lumens as the aorticopulmonary septum is pulled and rotated toward the heart by the retracting myocardium attached to aorticopulmonary prongs. The aortic sac is thereby divided into the base of the aorta and pulmonary trunk (Van Mierop, 1979). As development proceeds, the mesenchyme distal to the myocardial edge condenses to form the tunica media at the base of these vessels while the tissue proximal to the myocardial rim always develops into nascent semilunar valves (Thompson and Fitzharris, 1979, 1985). Collectively, these tissues become translocated toward the heart even though they develop autonomously. While this model claims no transformation of myocardium into vascular smooth muscle, it does not describe the origin of the mesenchyme distal to the myocardial rim of the truncus (Thompson and Fitzharris, 1979).

In this paper, we report that the secondary heart field, which was previously reported to provide the myocardium for the lengthening of the distal cardiac outflow tract, also gives rise to the smooth muscle at the myocardial–arterial junction where the semilunar valves form. Because the secondary heart field gives rise to both the myocardium and smooth muscle, we have called this region the arterial pole. The designation “arterial pole” has recently been associated with anterior heart field which also gives rise to the right ventricle and conotruncus (Kelly et al., 2001), but it is more appropriate to confine the designation to the junction of the ventricular myocardium with the smooth muscle tunics of the great arteries. The smooth muscle tunic at the base of the aorta and pulmonary trunk is derived from cells originating in the secondary heart field proximally, and these cells join a more distal smooth muscle tunic derived from neural crest cells. The only neural crest at the base of the outflow tract is in the medial walls of the arterial trunks continuous proximally with the remnant of the aorticopulmonary septum. These data indicate that there are two “seams” at the arterial pole, i.e. the myocardial-to-smooth muscle junction derived from the secondary heart field at the base of the arterial trunks, and the junction of the secondary heart field-derived smooth muscle with cardiac neural crest-derived smooth muscle. Significantly, these seams are focal points for dissecting lesions of the aorta such as those seen in Marfan’s syndrome.

Materials and methods

Animal preparation

Fertilized chicken eggs, obtained from the Gold Kist Hatchery, Siler City, NC, were incubated at 37°C and 70% humidity in a forced-draft incubator. Embryos were harvested at suitable times for the analysis. For all of the secondary heart field marking studies, stage 14 chick embryos were placed in shell-less culture as described previously (Yelbuz et al., 2002).

Chimeras

Quail-to-chick chimeras were prepared as described previously (Waldo et al., 1998). The chick embryo was the host and the quail embryo was the donor in each case. A total of 12 embryos was collected at Hamburger and Hamilton (1951) stages 22, 24, 26, 28 and incubation day 11 and fixed in methacarn or phosphate buffered paraformaldehyde, sectioned sagittally and stained with quail cell perinuclear antibody (QCPN).

Secondary heart field cell tracing

Embryos were injected with a mixture of 5-carboxytetramethylrhodamine, succinimidyl ester (CRSE; Molecular Probes, Inc., Eugene, OR) and 1,1′-dioctadecyl-3,3,3′-tetramethylindocarbocyanine perchlorate (DiI; Molecular Probes, Inc.) as described previously (Darnell and Schoenwolf, 2000; Kirby et al., 2003). The embryos were photographed after the injection and at 4 h intervals thereafter. The embryos were fixed in 4% phosphate buffered paraformaldehyde and embedded in paraffin for immunohistochemistry.

Immunohistochemistry

Embryos were collected between stages 14 and 28 and fixed in methacarn, embedded in paraffin, sectioned at 8

μm and processed as described previously (Waldo et al., 1996, 1998, 2001). HNK1, MF20 and QH-1 were visualized with Alexa 568 goat anti-mouse IgG conjugate (Molecular Probes). The QCPN was obtained from the Developmental Studies Hybridoma Bank, University of Iowa, Iowa City, IA. Embryos injected with DiI/CRSE were embedded in paraffin, sectioned and processed for immunohistochemistry using anti-rhodamine conjugated, rabbit IgG polyclonal antibody (Molecular Probes, Inc.) as described previously (Kirby et al., 2003).

In situ hybridization

The 680 bp fragment of SM22 (accession number M83105) was generated by RT-PCR using primers spanning 143–803 bp and cDNA from stage 22 chick embryos. The cDNA fragment was cloned into pCRII (Invitrogen). PCR fragments containing one of the promoter primers and one of the gene specific primers were generated and labeled with digoxigenin. An Nkx2.5 digoxigenin-labeled riboprobe was generated from a 221 bp fragment of the chick Nkx2.5 cDNA as previously described (Waldo et al., 2001). After examination and documentation of whole-mount staining, the embryos were embedded, in 15% sucrose and 7.5% gelatin, frozen and cryo-sectioned at 12 μm and mounted.

Results

The smooth muscle at the base of the aorta and pulmonary trunk is not derived from cardiac neural crest

Quail-to chick chimeras (total of 4 harvested between days 11–18 of incubation) were generated to establish the location of cardiac neural crest cells relative to the myocardial–smooth muscle junction of the arterial pole. At day 11, the tunica media at the base of both the aorta and the pulmonary trunk (arrows in Figs. 1A, B) contained no cardiac neural crest cells (Fig. 1B). Distally, the tunica media of both vessels consisted entirely of quail cardiac neural crest cells (brown cells in Fig. 1B), whereas in a transitional area between the proximal and distal part of the outflow vessel walls, there was a shift from non-neural crest to neural crest cells forming what we will refer to as a seam (arrowheads in Fig. 1B). Both the proximal and distal walls of the aorta and pulmonary trunk consisted of vascular smooth muscle as indicated by α smooth muscle actin (αSMA)-positive staining (green) in Fig. 1C. Myocardial tissue, positive for MF20, interdigitated with vascular smooth muscle, positive for αSMA, in the region of the sinuses. These results show that the tunica media of the outflow vessels is derived from two populations of vascular smooth muscle cells, one of which is cardiac neural crest-derived and the other from an as yet unknown source. We used quail–chick chimeras to rule out the possibility that the non-neural crest cells could be provided by neural crest from a more cranial or caudal level (data not shown).

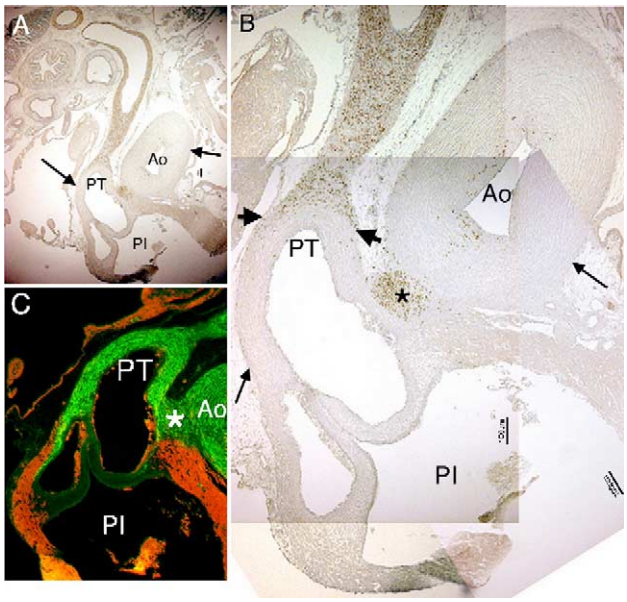

Fig. 1. Smooth muscle at the base of the aorta and pulmonary trunk is not derived from cardiac neural crest. Day 11 quail-to-chick chimera stained with QCPN (brown) to label quail cardiac neural crest cells, MF20 (red) to label myocardium and alpha SMA (green) to label the vascular smooth muscle. (A) Low magnification of a frontal section of the pulmonary trunk (PT), pulmonary infundibulum (PI) and a cross-section of the proximal part of the aorta (Ao). (B) Composite of panel (A) at higher magnification. The proximal walls of the PT and the aorta (arrows) are composed of non-cardiac neural crest cells (chick) while the distal part of the pulmonary trunk is composed of neural crest cells (brown quail cells). Arrowheads mark the transition from quail cardiac neural crest cells to chick non-cardiac neural crest cells. Remnant of the neural crest-derived aorticopulmonary (AP) septum (*). (C) The base of the PT consists of a non-neural crest cell population expressing alpha SMA but not MF20. The wall of the PI is myocardial. Red staining lining the valve leaflets is autofluorescence from blood cells. Scale bars = 100 μm.

Two populations of cells originate in the secondary heart field to provide myocardium and smooth muscle to the arterial pole

To obtain a more precise record of cells originating from the secondary heart field and to determine whether this region is the source of the non-neural crest-derived smooth muscle at the arterial pole, we labeled cells from the secondary heart field as they moved into the outflow tract using a mixture of DiI/rhodamine. The DiI/rhodamine was microinjected into the secondary heart field of chick embryos at stages 14–15 (n = 54; Figs. 2A–D) and 18–20 (n = 25; Figs. 2E–H). We found cells moving into the arterial pole in two temporally separated groups. The first group of cells, marked at stage 14–15, migrated to the distal outflow myocardium and differentiated into myocardial cells (Figs. 2C, D). These cells migrated in a spiral manner ending on the contralateral side of the outflow tract, that is, cells marked in the right side of the secondary heart field

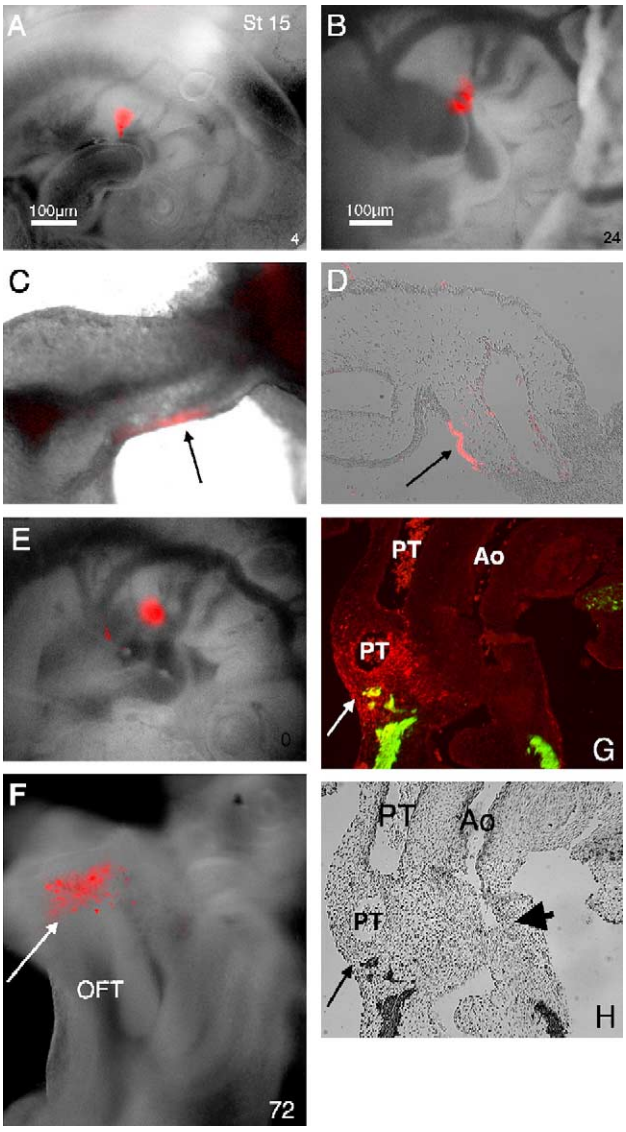

Fig. 2. The secondary heart field provides myocardium and smooth muscle cells to the arterial pole. Cells of the secondary heart field were labeled at stage 15 (A–D) and stage 18 (E–H) with a mixture of DiI and rhodamine (red). (A) 4 h after injection at stage 15; labeled cells are located in the ventral floor of the pharynx caudal to the outflow tract. (B) 24 h after injection; labeled cells translocated to the base of the outflow tract. (C) Stage 22 heart 48 h after right secondary heart field injection; left view of the outflow shows labeled cells located in the distal outflow myocardium (arrow) on the left side. (D) Section through outflow of heart in panel (C) stained with anti-rhodamine. Labeled cells are incorporated into the myocardial wall (arrow). (E) Injection at stage 18 (right side labeled); labeled cells are caudal to the distal outflow tract. (F) 72 h after injection (stages 27–28) view from the dorsal (posterior) side of the heart; labeled cells are in the smooth muscle wall of the arterial pole dorsal to the distal outflow tract (OFT) (arrow). (G) Section through outflow of embryo in panel (F) stained with anti-rhodamine (red) anti-MF-20 (green); rhodamine-labeled cells are located in the wall of the base of the pulmonary trunk (PT, arrow) and not in the myocardium. Ao = aorta. (H) The section in panel (G) was restained with anti-αSMA (black) to show vascular smooth muscle in the walls of the aorta (Ao) and pulmonary trunk (PT). The rhodamine-labeled cells in the base of the pulmonary trunk in panel (G) were not yet expressing αSMA (arrow) even though the distal wall of the pulmonary trunk was αSMA-positive. The proximal aortic wall was just initiating expression of αSMA as shown in Fig. 1 (arrowhead).

ended up on the left side of the arterial pole. As development proceeded, the outflow tract joined the pharynx at progressively more caudal levels. This suggests that the first group of cells derived from the secondary heart field is incorporated into the myocardium of the arterial pole as the outflow moves caudally.

The second group of cells, marked in embryos at stages 18–20 (Fig. 2E), was added to the ipsilateral side of the outflow by "dropping" from a horizontal plane behind the outflow tract to a vertical plane displacing the myocardial rim toward the heart. The majority of these cells was not positive for MF20 and formed the caudal wall of the aortic sac above the myocardial rim (thin arrows in Figs. 2F, G, H). We will refer to the junction of the distal myocardial rim with the non-myocardial cells at this ventriculoarterial junction as the first seam. Thus, the first seam is formed by the transition in differentiation of myocardial to non-myocardial cells from the secondary heart field and is a seam between two cell types derived from the same progenitor population, i.e. secondary heart field.

The secondary heart field maintains a similar appearance and expresses Nkx2.5 in both the myocardial and non-myocardial progenitor populations

The secondary heart field is morphologically distinct as a pseudostratified columnar layer of epithelial cells. This morphology was maintained from early looping stages (stage 14) until initiation of outflow tract septation (stage 26). This layer was the thickest at the bend between the pericardial roof and the distal outflow tract and varied only slightly during the times that the two groups of secondary heart field cells were added either to the outflow tract or to the aortic sac region. For example, at stage 16, when myocardial cells migrate from the secondary heart field into the outflow tract, the depth of the layer averaged 37 μm ($n = 6$) at its thickest point (Fig. 3), but at stage 19 after the myocardial component of the secondary heart field had been added to the outflow, its thickness was reduced to an average of 21 μm ($n = 6$) (Figs. 3A, D, K). From stages 22–24, when smooth muscle precursors move from the secondary heart field into the aortic sac wall, its thickness averaged 31 μm at stage 22 (84% of its thickness at stage 16; $n = 6$) (Figs. 3E, K) and 26 μm at stage 24 ($n = 6$) (Figs. 3H, K). It was not until stage 26/27, when septation of the outflow tract was initiated, that the thickness of the secondary heart field dwindled to a 10 μm thick single layer of cells (Figs. 3I, J, K). As we have already reported (Waldo et al., 2001), the secondary heart field expressed Nkx2.5 during looping (Figs. 3B, C). Even after the myocardial component had added to the outflow, the secondary heart field continued to express Nkx2.5 in the region of the aortic sac suggesting that the smooth muscle progenitor population retained myocardial potential. This was the case at stage 22 when the smooth muscle progenitors derived from secondary heart field were moving into the aortic sac wall (Figs. 3F, G).

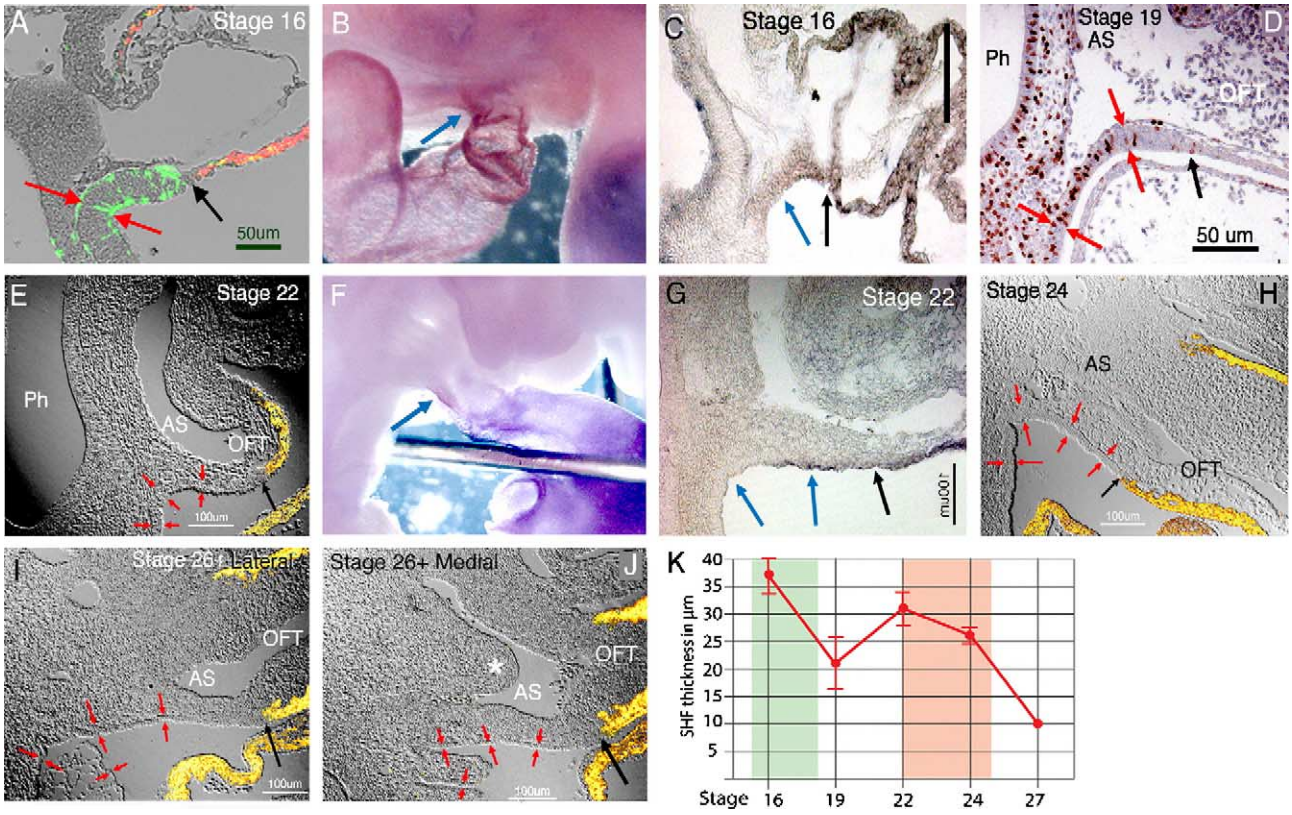

Fig. 3. The appearance of the secondary heart field is similar over time until outflow septation begins. Sagittal sections of the secondary heart field at stage 16 (A, C), stage 19 (D), stage 22 (E, G), stage 24 (H) and stage 26/27 (I, J). At all stages except 26/27, the secondary heart field consists of a thickened layer of pseudostratified columnar epithelial cells that are widest at the bend between the pericardial roof and distal outflow tract. By late stage 26, this epithelium has thinned dramatically. (A) HNK-1 (green) labels the pseudostratified columnar epithelial layer of the secondary heart field cells that averages 37 μm at its thickest point (between red arrows). Black arrow shows the junction of the secondary heart field and distal myocardium stained by MF20 (red). (B) Nkx2.5 messenger RNA is expressed in the secondary heart field (blue arrow) at stage 16. (C) Frozen sagittal section of the secondary heart field of the embryo in panel (B). Nkx2.5 is expressed in the secondary heart field epithelium (blue arrow) that is continuous with the distal outflow tract myocardium (black arrow). (D) Section of the secondary heart field was immunostained with antiBrdU (dark nuclei) to mark proliferating cells and counterstained with hematoxylin (blue). The secondary heart field now averages 21 μm at its thickest point (between red arrows). (E) The secondary heart field averages 31 μm at its thickest point (between red arrows) and is still a pseudostratified columnar epithelium (between red arrows). (F) Nkx2.5 is still expressed in the secondary heart field at stage 22 even though the outflow tract is no longer lengthening. Blue arrow = Nkx2.5 messenger RNA expression in caudal region of the aortic sac. (G) Stage 22 frozen sagittal section. Nkx2.5 messenger RNA is expressed in the secondary heart field epithelium adjacent to the aortic sac region (blue arrow) and is continuous with the outflow tract myocardium (black arrow). (H) The secondary heart field averages 26 μm at its thickest point (between red arrows). (I, J) As outflow septation is initiated, the secondary heart field has changed from pseudostratified to a simple cuboidal epithelium. It measures about 10 μm at its thickest point (between red arrows). Black arrows indicate junction of myocardium stained with MF20 (yellow) with the wall of the nascent outflow artery. (K) The average thickness of the secondary heart field epithelium remains relatively constant during the periods when secondary heart field cells are added to the myocardium and the aortic sac and declines afterward. Green shading indicates stages when myocardial cells are added to the outflow tract. Red shading indicates stages when smooth muscle cells are added to the aortic sac region.

Identification of the non-myocardial cell population derived from the secondary heart field

Embryos were collected from stages 14 to 26 (n = 57) and stained as whole mounts with MF20 to visualize the junction of the myocardium with the vascular smooth muscle walls of the aortic sac. From stages 14 through 20, the myocardial rim abutted the roof of the pericardial cavity and was relatively straight (arrows in Fig. 4A). This is the period when myocardium is added to the outflow tract from the secondary heart field. Between stages 22 and 26, the non-myocardial cells in the caudal wall of the aortic sac formed a lengthening gap between the roof of the pericardial cavity and the myocardial rim (asterisks in Fig. 4B). This time interval corresponded to the period when the second group of labeled cells moved from the secondary heart field. As the non-myocardial cells were added, the myocardial rim gradually changed from flat to saddle-shaped with two peaks laterally separated by a cranial and a caudal depression (Bartelings and Gittenberger-de Groot, 1989) (dotted line in Fig. 4B).

To further delineate the myocardial-to-non-myocardial junction in stages 22–27 embryos, we examined SM22 expression (n = 12). SM22 is an early marker of vascular smooth muscle. At stages 22 and 24, all of the mesenchyme in the aortic sac region expressed SM22 (areas between arrowheads in Figs. 5A–E) and was complimentary to the saddle shape of the myocardial rim (dotted lines

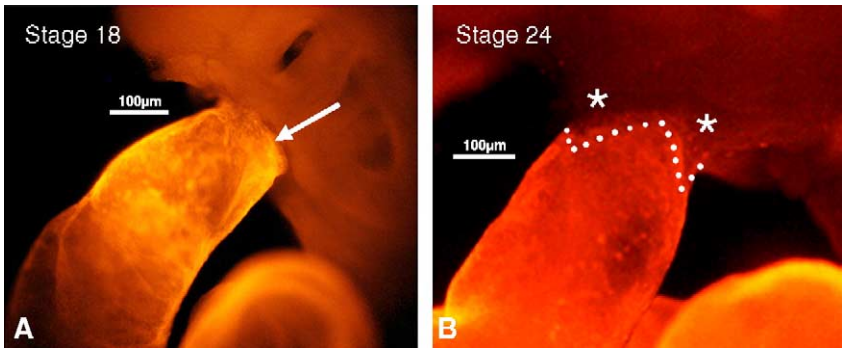

Fig. 4. Myocardial-to-smooth muscle junction of the arterial pole. Whole mount embryos stained for MF20 (red) to distinguish the distal myocardial edge from the smooth muscle wall of the aortic sac. (A) At stage 18, the myocardial rim was flat (arrow). (B) By stage 24, the myocardial rim has begun to retract, as the aortic sac (asterisks) extends into the distal outflow (scale bars = 100 μm).

in Fig. 3B). By stage 27, SM22 was differentially expressed in the left and right mesenchyme ensheathing the aortic sac (thick arrows in Figs. 5F–H). There was intense SM22 expression in the mesenchyme immediately adjacent to the myocardial cuff (thin arrows in Figs. 5F–H). These results suggest that the non-myocardial cells derived from the secondary heart field distal to the myocardial rim are probably the precursors of the vascular smooth muscle cells that will form the tunica media at the base of the great arteries.

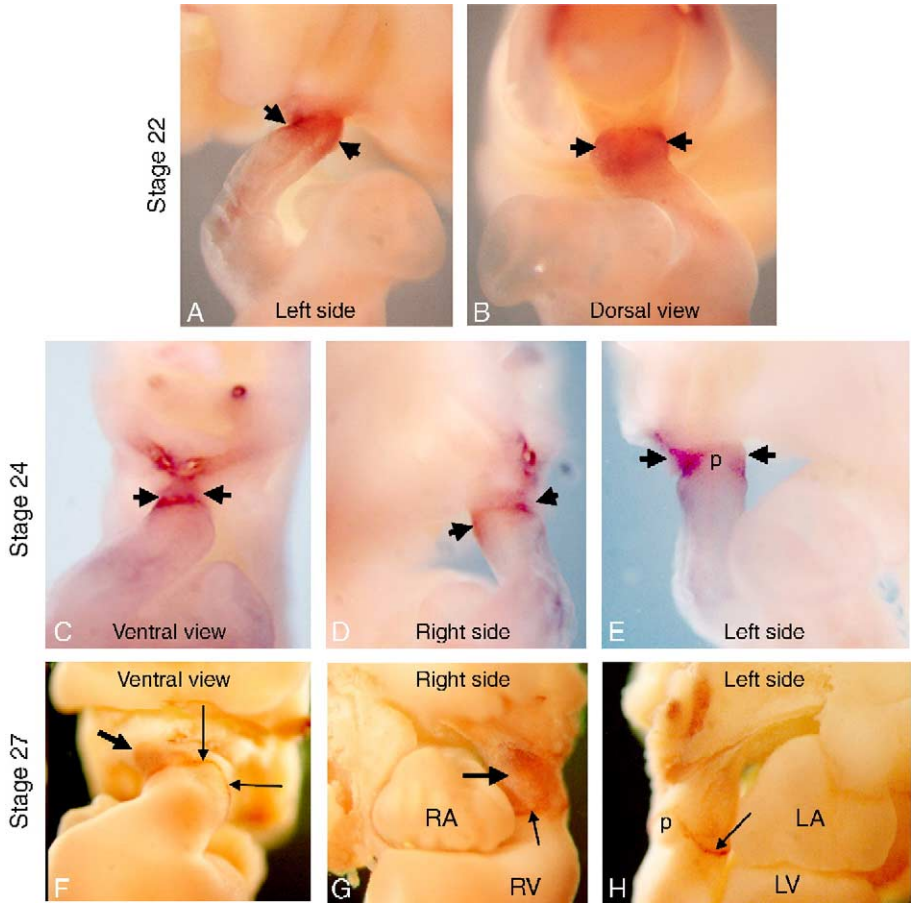

Fig. 5. Myocardial–smooth muscle junction at stages 22–27. Whole mount in situ hybridization showing SM22 expression in the arterial pole at stages 22 (A–B), 24 (C–E) and 27 (F–H). (A, E and H) Left view of the distal outflow tract and the aortic sac region. (B) Dorsal view of the distal outflow tract and the aortic sac. (C, F) Ventral view of the outflow tract and aortic sac region. (D, G) Right view of the distal outflow tract and the aortic sac region. p = myocardial peak. (A–E) At stages 22 and 24, the SM22-positive mesenchyme (between the arrowheads) sheaths the aortic sac. (F–H) By stage 27, expression of the SM22 is stronger in the mesenchyme surrounding the aortic sac on the right (thick arrow in panels F and G) and is intensely expressed in mesenchyme adjacent to the myocardial edge (thin arrows). RA, LA = right and left atrium. RV, LV = right and left ventricle.

Expression of other vascular smooth muscle markers during the development of the arterial pole

To further examine the smooth muscle progenitor population derived from the secondary heart field, we stained with antibodies for αSMA and myosin light chain kinase (MLCK) (n = 36; Fig. 6), which has been reported to be one of the earliest markers of smooth muscle differentiation (Yablonka-Reuveni et al., 1998). αSMA has been previously reported to be expressed by neural crest-derived smooth muscle in the aortic arches and in the aorticopulmonary septum (Beall and Rosenquist, 1990; Ya et al., 1997).

Throughout all the stages examined, both αSMA and MLCK were localized to the cells ensheathing the aortic arch arteries (Figs. 6A, H) and the roof of the aortic sac (Figs. 6B, H). αSMA- and MLCK-positive neural crest cells migrated into the cardiac jelly underneath the outflow myocardium (long arrow, Figs. 6A, H). αSMA, MLCK and MF20 were consistently coexpressed in the outflow tract myocardium up to stage 28 when expression of both smooth muscle markers was lost in all but the most distal myocardial rim. The smooth muscle cells derived from the secondary heart field did not express αSMA or MLCK at stages 22–27 and could be identified by their lack of expression of either marker (arrowhead in Figs. 6B, H). As the walls of the aortic sac elongated, this vascular smooth muscle-negative gap remained associated with the myocardial rim and the more distal αSMA-positive cells remained in the distal aortic sac walls.

The aortic sac was divided by the aorticopulmonary septum (asterisk, Fig. 6C) into systemic and pulmonary channels at stage 26 (Fig. 6C). By stage 28, the aorticopulmonary septum had entered the distal truncus (asterisk in Fig. 6E). The αSMA-negative gap observed at earlier stages in the caudal wall of the aortic sac (arrowhead in Fig. 6B) was now αSMA-positive at the base of the nascent aorta and pulmonary trunk (arrows in Figs. 6D, F). This region corresponded to the final destination of the

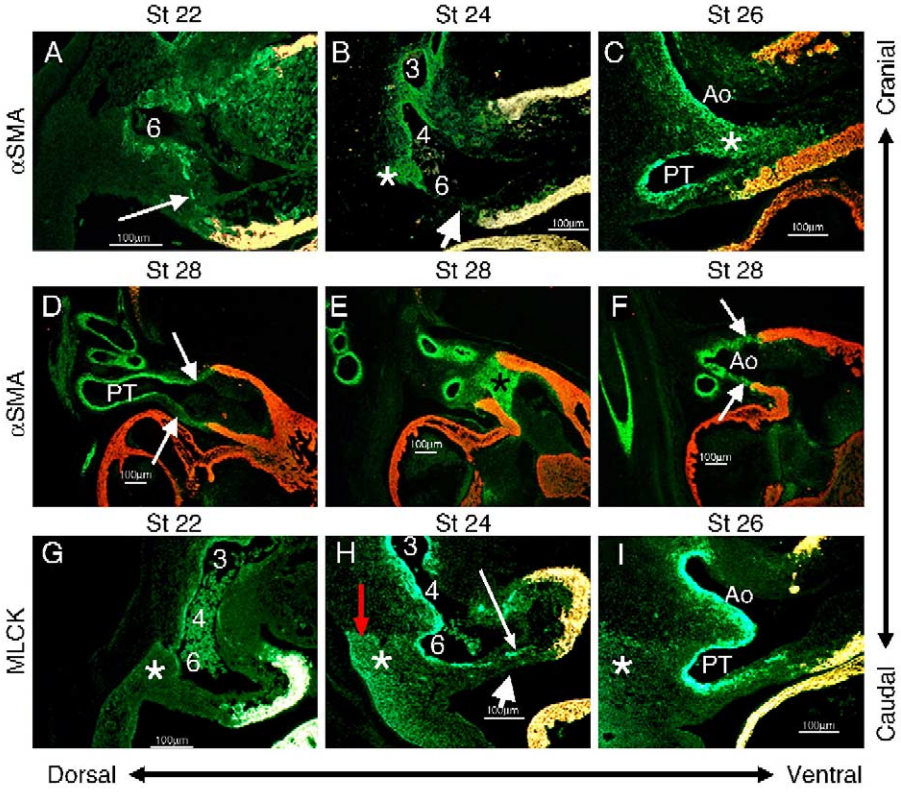

Fig. 6. Expression of smooth muscle markers during arterial pole development. αSMA (green, A–F), MLCK (green, G–I) and MF20 (red, A–I). Yellow or white indicates coexpression of MF20 and αSMA or MLCK. Sagittal sections from stages 22 (A, G), 24 (B, H), 26 (C, I) and 28 (D–F). (A) arrow = line of αSMA-positive cells extending from base of the sixth (6) arch artery to the distal myocardial cuff. (B) arrowhead = αSMA-negative gap in caudal wall of aortic sac; * = αSMA-positive mesenchyme will form the mid-part of the aorticopulmonary septum in roof of aortic sac between arch arteries 4 and 6. 3, 4, 6 indicate where these arch arteries branch from the aortic sac. (C) * = aorticopulmonary septum. Ao = aorta. PT = pulmonary trunk. (D) Arrows = proximal part of the pulmonary trunk; was originally an αSMA-negative gap in caudal wall of the aortic sac at stage 24 (arrow in panel B). (E) * = mid aorticopulmonary septum. (F) arrows = proximal part of aortic walls now expressing αSMA. (G) * = MLCK-positive mesenchyme adjacent to aortic sac. (H) * = MLCK-positive mesenchyme between the aortic sac and foregut endoderm. Red arrow = sharp cranial edge of MLCK-positive mesenchyme. Arrowhead = MLCK-negative caudal wall of the aortic sac. Long white arrow = αSMA-positive cells migrating from wall of aortic arch artery 6 into the distal outflow tract. (I) The aortic sac is being divided into the aorta (Ao) and the pulmonary trunk (PT) by the aorticopulmonary septum between the two outflow vessels. * = MLCK-positive mesenchyme. All scale bars in this figure = 100 μm.

second group of marked secondary heart field cells. Expression of αSMA was initiated within the gap (arrows in Figs. 6D, F) so that the walls of the aorta and pulmonary trunks were expressing αSMA along their entire length by stage 28 or 29.

MLCK was differentially expressed in the mesenchyme around the aortic sac (Fig. 6G). An abrupt line of MLCK staining could be seen between the origin of the 6th and 4th aortic arch arteries from the aortic sac (red arrow in Fig. 6H). This line coincided with the position where the aorticopulmonary septum began to bulge into the aortic sac at stage 24 (asterisk in Fig. 6B). MLCK expression was the strongest adjacent to the foregut floor and diminished in intensity near the roof of the aortic sac (Figs. 6H, I). In quail–chick chimeras, the neural crest cells stopped abruptly where the line of MLCK expression was highest on the right side and mid-aortic sac region (Figs. 7C–F).

In summary, these results show that differentiation of the cells from a nascent vascular smooth muscle SM22-positive population to definitive vascular smooth muscle occurred after the aortic sac had been divided by the aorticopulmonary septum at stages 28–29. αSMA, a contractile protein required for smooth muscle function, was expressed late in the smooth muscle cells derived from the secondary heart field even though it is present in smooth muscle derived from cardiac neural crest much earlier. In fact, smooth muscle derived from secondary heart field is recognizable as a gap between the myocardial rim and the αSMA-positive neural crest-derived smooth muscle. We refer to this population as secondary heart field-derived vascular smooth muscle. By contrast, MLCK, which is thought to be one of the earliest markers of smooth muscle differentiation, was not expressed by smooth muscle derived from secondary heart field at the stages examined. Finally, differential expression of MLCK in the mesenchyme around the caudal aortic sac marks the region just caudal to the origin of the neural crest-derived aorticopulmonary septum in the aortic sac.

Cardiac neural crest at the arterial pole

Quail-to-chick chimeras (n = 12) were generated to observe cardiac neural crest cells during the development of the arterial pole. During stages 22–24, cardiac neural crest cells ensheathed the caudal arch arteries (not shown) and migrated into the cardiac jelly adjacent to the distal outflow tract myocardium (Supplementary Fig. 1). The smooth muscle precursors derived from the secondary heart field were represented by an αSMA-negative gap in the caudal wall of the mid-aortic sac which was also QCPN-negative (arrow in Figs. 7A, B). Cardiac neural crest cells filled the mesenchyme between the roof of the aortic sac and the foregut endoderm (Fig. 7A). Cranially, these crest cells ended abruptly at the thyroid primordium (T) and caudally at the junction of the sixth aortic arch artery with the aortic

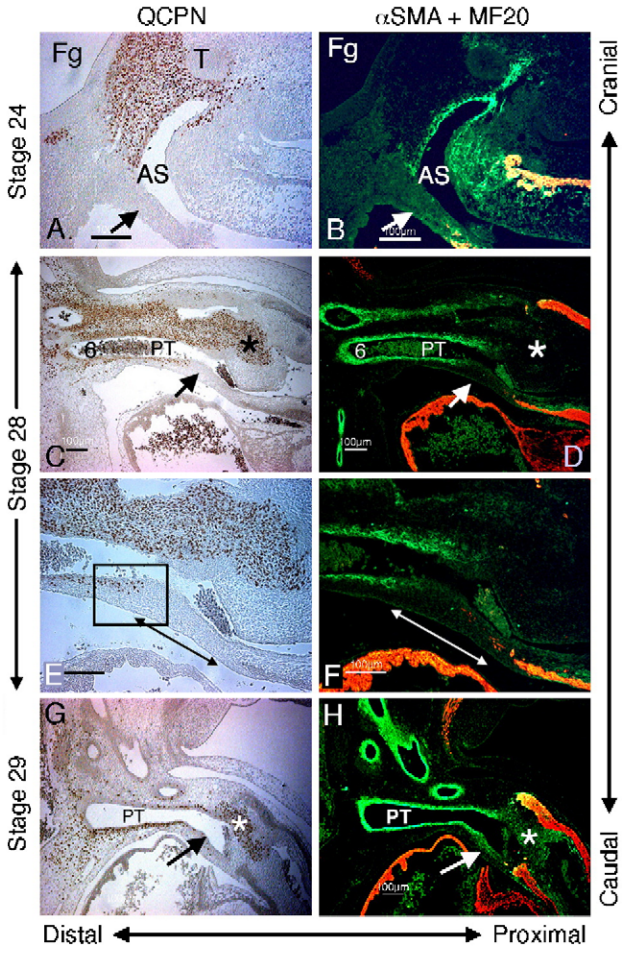

Fig. 7. Cardiac neural crest cells form the tunica media distal to the cells derived from the secondary heart field. Sagittal sections of quail/chick chimeras were labeled with QCPN to identify quail cardiac neural crest cells (brown in panels A, C, E, G). Myocardial cells are MF20-positive (red); smooth muscle cells are αSMA-positive (green) and yellow indicates coexpression of MF20 and αSMA (B, D, F, H). (A–B) Stage 24. (C–F) Stage 28. (G–H) Stage 29. (A, B) Mid-aortic sac region. An αSMA-negative gap in the caudal wall of the aortic sac (AS) is cardiac neural crest-free (arrow). Fg = foregut, T = thyroid gland. (C–F) Stage 28. The aorticopulmonary septum (*) has divided the aortic sac into the aorta and pulmonary trunks. PT = pulmonary trunk. The smooth muscle-negative gap seen in the caudal wall of the aortic sac at stage 24 is now located proximally in the free wall of the pulmonary trunk distal to the edge of the myocardium and is composed mainly of chick cells (arrow in panels C, D, G, H). Distally, the remainder of the free wall of the pulmonary trunk consists of cardiac neural crest cells. (E, F) High magnification of smooth muscle-negative gap in panels C and D. The double-headed arrow delineates the secondary heart field-derived part of the tunica media of the pulmonary trunk. A seam is formed in the tunica media of the free wall at the point where the cardiac neural crest cells meet the chick cells (box in panel E). (G, H) By stage 29, expression of αSMA is initiated (Supplement, Fig. 2) in the area that had been previously smooth muscle actin-negative. All scale bars in this figure = 100 μm.

sac (Fig. 7A). Only those crest cells that were in the roof and floor of the aortic sac expressed αSMA (Fig. 7B). At stage 24, the secondary heart field-derived vascular smooth muscle precursors in the caudal walls of the aortic sac were distal to the edge of the myocardial rim and did not express

αSMA. During subsequent stages, the aortic sac lengthened as the aorticopulmonary septum divided the aortic sac into aortic and pulmonary trunks (Supplementary Fig. 2). This lengthened the region of secondary heart field-derived smooth muscle precursors that continued to be negative for αSMA expression. By stages 28–29, aorticopulmonary septation of the aortic sac was complete and the secondary heart field-derived smooth muscle was beginning to express αSMA (arrows in Figs. 7C, D, G, H). The medial (facing) walls of the aorta and pulmonary trunk consisted entirely of cardiac neural crest cells continuous with the aorticopulmonary septum in the truncus (* in Figs. 7C, G). Distally, the remainder of the free walls was comprised entirely of αSMA-positive cardiac neural crest cells. A seam formed (box in Fig. 7E) where the quail cardiac neural crest cells interfaced with the chick non-neural crest cells. In succeeding days up to embryonic day 18 (data not shown), the base of the aorta and pulmonary trunk continued to be neural crest-free except in the adjoining walls.

We conclude from these data that the tunica media of the aorta and pulmonary trunk is made of populations of smooth muscle cells derived from two sources: cardiac neural crest distally and secondary heart field proximally.

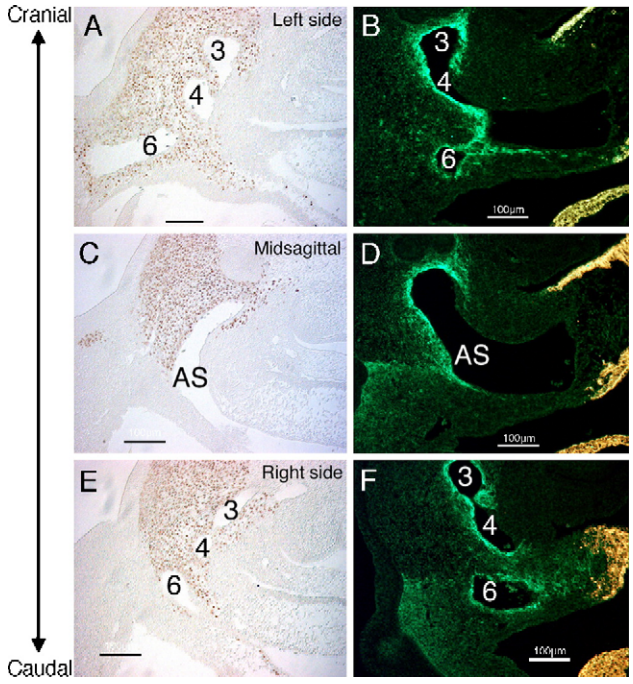

Fig. 8. The cranial border of MLCK expression corresponds with the caudal border of cardiac neural crest ectomesenchyme destined to form the aorticopulmonary septum. (A, C, E) Stage 24 quail–chick chimera stained with QCPN antibody (brown) to identify quail cardiac neural crest cells. (B, D, F) Stage 24 chick embryo labeled with MF20 (red, myocardium) and MLCK (green, vascular smooth muscle). Yellow indicates coexpression of MF20 and MLCK. (A, B) Left side of the embryo at the point where the base of the three caudal arch arteries (3, 4, 6) join the aortic sac. Neural crest cells ensheath the 6th arch artery and nearly surround the 3rd and 4th arch arteries. MLCK is not expressed in the mesenchyme between the roof of the aortic sac and the pharyngeal floor except in the subendothelial cells of the aortic sac. (C, D) Midline of the aortic sac (AS). The cranial edge of MLCK expressing tissue borders the caudal edge of ectomesenchyme between the floor of the pharynx and the roof of the aortic sac. (E, F) Right side. All scale bars in this figure = 100 μm.

Discussion

Secondary heart field marking studies show that there are two groups of secondary heart field cells that undergo separate periods of migration into the arterial pole. The first group migrates to the distal outflow tract where the cells differentiate into myocardium. After outflow myocardial elongation is complete, a second group of cells moves into the aortic sac region. Concurrently, the aortic sac lengthens and is invested by SM22-positive, αSMA- and MLCK-negative cells that appear as the myocardial cuff regresses. We have called these cells secondary heart field-derived vascular smooth muscle progenitors. Quail–chick chimeras confirm that neural crest cells do not enter this region. Over time, the secondary heart field-derived smooth muscle progenitors remain associated with the distal rim of the myocardium as the aortic sac lengthens and is septated by the aorticopulmonary septum into the nascent aorta and pulmonary trunk. A seam is formed where the αSMA-positive neural crest cells meet the secondary heart field-derived vascular smooth muscle progenitors. It is only after septation of the aortic sac is complete that the secondary heart field-derived vascular smooth muscle begins to express αSMA indicating that these secondary heart field-derived cells are differentiating into vascular smooth muscle.

The smooth muscle at the base of the arterial pole is continuous with the cardiac neural crest-derived smooth muscle. Le Lièvre and Le Douarin (1975) originally showed that the great arteries are enveloped in a smooth muscle tunic derived from neural crest cells. Kirby et al. (1983) later showed that the neural crest originating from the rhombencephalon between the mid-otic placode and somite 3, called cardiac neural crest (Kirby et al., 1985), provides cells that comprise the aorticopulmonary septum, in addition to the vascular smooth muscle cells in the tunics of the great arteries. Waldo et al. (1994), in a study of the developing coronary arteries, noted that the vascular smooth muscle cells at the base of the aorta and pulmonary trunks were not comprised of cardiac neural crest cells, but it was not clear where these cells originated. This study shows that the myocardium proximal to the semilunar valves and the vascular smooth muscle cells distal to the semilunar valves are both derived from the secondary heart field which was originally described to contribute only myocardium to the outflow tract (Mjaatvedt et al., 2001; Waldo et al., 2001). Interestingly, deVries reported that the "pharyngeal mesenchyme" which we have referred to as secondary heart field contributes to the cardiac outflow tract over two decades ago (deVries, 1981). However, his observation was not based on cell movements but was inferred from histological sections. The more recent

marking studies in pharyngeal mesenchyme have investigated the myocardial potential and movement of the cells into the outflow tract.

The method of addition of cells to the arterial pole and lengthening of the aortic sac described here is in agreement with the model of arterial pole development proposed by Thompson and Fitzharris (1979) but is in contrast to the model of outflow septation proposed by Anderson et al. (2003, review). Our current model of addition of secondary heart field to the outflow tract, based on cell tracing and expression studies, is shown in Fig. 9. The myocardium is added to the distal outflow tract between stages 14–20. The smooth muscle component of the proximal part of the aorta and pulmonary trunk is added by the secondary heart field between stages 22 and 28, concurrent with the initiation of outflow tract septation by the aorticopulmonary septum through an elongated aortic sac into the truncus. In contrast, Anderson and colleagues, using histological sections of rat, mouse and human embryos do not believe that the intrapericardial portion of the aorta and pulmonary trunk are derived from an elongated aortic sac. Instead, they propose that the myocardial walls of the distal outflow tract (truncus) undergo a myocardial-to-arterial smooth muscle transformation to become the intrapericardial tunic of the aorta and pulmonary trunk (reviewed in Anderson et al., 2003). This process is proposed to occur simultaneously as the distal outflow tract is septated by fused truncal cushions rather than an aorticopulmonary septum. On the other hand, Jiang et al. (2000), who created the Wnt1-Cre transgenic mouse in order to label cardiac neural crest cells during heart development, showed that the proximal part of the aorta and pulmonary trunk were composed of both neural crest cells and smooth muscle from an unknown source. Although their emphasis was not on the development of the arterial smooth muscle, they suggested that these smooth muscle cells were derived from the pharyngeal tissue near the trachea. We believe that, in the mouse, these cells could be derived from the secondary heart field as they are in the chick. Neural crest cell tracing in conditional mouse models such as the Wnt1-cre, the Pax3-Cre, the P0-Cre and the Cx43-Lacz mouse (Epstein et al., 2000; Jiang et al., 2000; Li et al., 2000; Waldo et al., 1999; Yamauchi et al., 1999) have clearly documented the formation of the aorticopulmonary septum by cardiac neural crest cells and have highlighted the role played by the aorticopulmonary septum in normal outflow tract development. Formation of the aorticopulmonary septum and septation of the truncus has also been documented by Kirby lab using markers of cardiac neural crest cells in quail/chick chimeras (Kirby et al., 1983, 1985; Miyagawa-Tomita et al., 1991; Waldo et al., 1998). In spite of this,

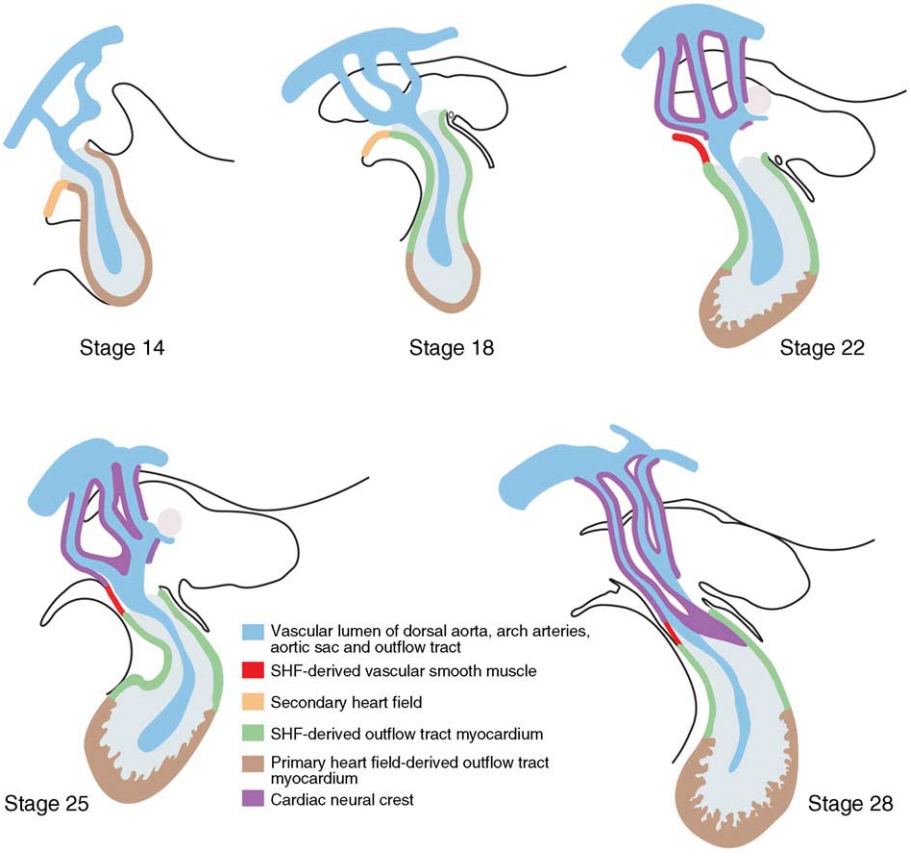

Fig. 9. Schematic diagram showing the timing/development of the myocardial and smooth muscle contributions to the arterial pole from the secondary heart field.

Anderson and colleagues fail to acknowledge septation of the aortic sac and the outflow tract by the neural crest-derived aorticopulmonary septum.

In our model, the myocardium of the truncus appears to remain at the level of the semilunar valves which are separated by the aorticopulmonary septum. Anderson and colleagues, on the other hand, state that the semilunar valves are derived from the distal aspect of the proximal outflow tract, just below the truncus which has now been transformed into the arterial walls of the outflow arteries. Chimeric studies show that the only neural crest cells seen at the level of the semilunar valves and distally for several hundred microns is the small remnant of the septation complex which persists as long as we have followed it to just before hatching. A similar situation appears to be the case in development of the mouse outflow tract although the details of secondary heart field contribution to the arterial pole remain to be determined (Jiang et al., 2000; Waldo et al., 1999).

Are the smooth muscle cells at the base of the great arteries derived from the secondary heart field or from a different population also located in the pharyngeal splanchnic mesoderm?

The mesenchymal layer in the pharyngeal floor caudal to the outflow tract which we have designated secondary heart field represents a continuous epithelial layer with the myocardium. This same layer of cells provides both myocardium to the distal outflow tract and smooth muscle to the base of the great arteries. Although we cannot show that both populations derive from the same progenitor cells, there are several reasons why we believe they may be the same population: first, at stage 22, the part of the secondary heart field epithelium adjacent to the aortic sac region still expresses Nkx2.5 even though the secondary heart field-derived myocardium has already been added to the outflow tract. At this stage, only the smooth muscle progenitors are located in this Nkx2.5-positive mesenchyme. If one considers Nkx2.5 expression to represent myocardial potential, it suggests that the smooth muscle progenitor population continues to have myocardial potential. Secondly, even after the secondary heart field no longer generates myocardial cells, this pseudostratified epithelium does not become simple cuboidal, as would be expected, and remains continuous with the same cells that differentiated as myocardium at earlier stages. The thickness varied only slightly (16%) when the myocardial (37 μm at stage 16) and prospective smooth muscle cells (31 mm at stage 22) were generated. It is not until stage 26/27, when outflow septation starts, that the pseudostratified secondary heart field epithelium begins to lose its pseudostratified appearance and thins into a single layer of epithelium signifying a change in activity by these cells. Third, the same collection of cells that we are calling secondary heart field cells undergoes similar waves of proliferation and HNK-1 expression but at different times.

While the progenitor cells for both myocardium and vascular smooth muscle at the arterial pole originate from the secondary heart field, we also believe that the two populations move into the arterial pole in different ways. The myocardium migrates into the contralateral side of the outflow tract in a spiraling manner. The smooth muscle progenitors move to the ipsilateral side of the arterial pole and are vertically displaced into the arterial wall. These separate processes are affected differently by cardiac neural crest ablation (Waldo et al., 2005).

Significance of MLCK expression

We used MLCK as a smooth muscle marker because it is reported to be the earliest definitive expression marker of smooth muscle (Yablonka-Reuveni et al., 1998). However, we were unable to detect MLCK expression in the vascular smooth muscle cells derived from the secondary heart field at the base of the aorta and pulmonary trunk at the stages we examined. We were surprised to find a line of MLCK positive to negative staining at exactly the site where the neural crest cells begin aorticopulmonary septation in the dorsal wall of the aortic sac between arch arteries 4 and 6. MLCK is a serine/threonine kinase that phosphorylates the regulatory light chain of myosin, resulting in increased contraction. In non-muscle cells, MLCK may regulate cell motility (Chew et al., 2002). Inhibition of MLCK causes a loss of actin stress fibers and focal adhesions, supporting a role for actin–myosin based contractility in maintaining these structures. Because of its role in tissue motility and adhesion, we hypothesize that the cells expressing MLCK form a border that initiates movement of neural crest cells into the aortic sac to form the aorticopulmonary septum (see Figs. 8A–F).

Significance of the junction of two different smooth muscle cell lineages at the base of the aorta

Aortic dissection is a difficult abnormality to diagnose and is the most common catastrophic condition affecting the aorta. Clinical diagnosis of aortic dissection necessitates immediate surgical repair (Finkelmeier and Marolda, 2001). Aortic dissections are frequently found at the aortic root and 2 cm above the aortic root (Jackeline Gomez-Jorge, MD eMedicine on line). These dissections are characteristic of Marfan's syndrome (Bharati and Lev, 1996). Our study shows the presence of two seams in the ascending aorta that are potential sites of aortic dissection. The first is the myocardial-to-smooth muscle transition at the semilunar valves which would coincide with dissection at the aortic root (Fig. 10). The myocardium and smooth muscle at this seam are both derived from the secondary heart field and it is not known what signals shift the fate of cells from myocardial to smooth muscle. These two cell types are interdigitated from their birth. The second seam is between the smooth muscle cells derived from the secondary heart

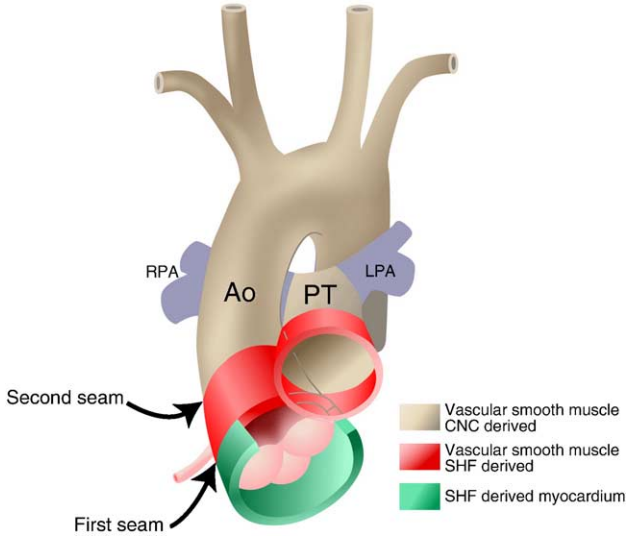

Fig. 10. Arterial pole of the human heart. The secondary heart field generates myocardium (green) and vascular smooth muscle (red). A seam is formed where the myocardial cells meet the vascular smooth muscle cells of the tunica media of the aorta and pulmonary trunk. The tunica media of the aorta and pulmonary trunk is derived from secondary heart field proximally (red) and the cardiac neural crest distally (tan). The interface between these populations creates a second seam. These seams are likely locations of aortic wall dissections.

field with those derived from the cardiac neural crest (Fig. 10). This seam corresponds with the second site of aortic dissection that is 2 cm above the aortic root. We have shown that, during development of the aortic root, the more distal neural crest-derived smooth muscle must find and interdigitate with the secondary heart field-derived smooth muscle to make a confluent tunica media. We speculate that these two seams are potentially weak sites that allow aortic dissection in abnormal conditions.

Importance to genetic models of understanding lineages derived from the secondary heart field

Several mouse models have defects in the development of the arterial pole. One of these is Tbx1 which is a DiGeorge candidate gene (Jerome and Papaioannou, 2001; Merscher et al., 2001; Vitelli et al., 2002; Yagi et al., 2003). Xu et al. (2004) have shown that in the mouse, *Tbx1* is expressed in secondary heart field progenitors where it regulates the addition of myocardium to the outflow. Loss of Tbx1 function results in fewer cardiomyocytes added to the outflow tract. Also implicated in the DiGeorge phenotype are Fgf8 and Shh (Abu-Issa et al., 2002; Frank et al., 2002; Garg et al., 2001). The exact cell populations that are affected in these mutants and many others are not well-defined, partly because of a lack of knowledge of the components that form the arterial pole during development. The findings reported in this paper help focus the analysis of these models on the varied cell lineages at the arterial pole to pinpoint those that are affected. For example, defects in the smooth muscle of the arterial pole can be a result of defective neural crest development, as has often been proposed, but in the light of the results presented in this paper, the defect can also, or alternatively, be related to cells derived from the secondary heart field. Finally, these data open the way to the analysis of the complex interactions and relationships among the different cell populations that make up the arterial pole.

Acknowledgments

We thank Ping Zhang for technical assistance. We are grateful to many colleagues who have participated in continuing discussions of this work and to Tony Creazzo and Erik Meyers for critical reading of the manuscript and many good suggestions. This work was supported by PHS grants HL36059, HL070140 and HD39946.

Appendix A. Supplementary data

Supplementary data associated with this article can be found, in the online version, at doi:10.1016/j.ydbio.2005.02.012.

References

Abu-Issa, R., Smyth, G., Smoak, I., Yamamura, K.-I., Meyers, E., 2002. Fgf8 is required for pharyngeal arch and cardiovascular development in the mouse. Development 129, 4613–4625.

Abu-Issa, R., Waldo, K.S., Kirby, M.L., 2004. Heart fields: one, two or more? Dev. Biol. 272, 281–285.

Anderson, R.H., Webb, S., Brown, N.A., Lamers, W., Moorman, A., 2003. Development of the heart: (3) formation of the ventricular outflow tracts, arterial valves, and intrapericardial arterial trunks. Heart 89, 1110–1118.

Arguello, C., de la Cruz, M.V., Sanchez, C., 1978. Ultrastructural and experimental evidence of myocardial cell differentiation into connective tissue cells in embryonic chick heart. J. Mol. Cell. Cardiol. 10, 307–315.

Bartelings, M.M., Gittenberger-de Groot, A.C., 1989. The outflow tract of the heart—Embryologic and morphologic correlations. Int. J. Cardiol. 22, 289–300.

Beall, A.C., Rosenquist, T.H., 1990. Smooth muscle cells of neural crest origin form the aorticopulmonary septum in the avian embryo. Anat. Rec. 226, 360–366.

Bharati, S., Lev, M., 1996. The Pathology of Congenital Heart Disease. Futura Publ. Co, Armonk, NY, pp. 1189–1210.

Chew, T.L., Wolf, W.A., Gallagher, P.J., Matsumura, F., Chisholm, R.L., 2002. A fluorescent resonant energy transfer-based biosensor reveals transient and regional myosin light chain kinase activation in lamella and cleavage furrows. J. Cell Biol. 156, 543–553.

Darnell, D.K., Schoenwolf, G.C., 2000. Culture of avian embryos. Methods Mol. Biol. 135, 31–38.

deVries, P., 1981. Evolution of precardiac and splanchnic mesoderm in relationship to the infundibulum and truncus. In: Pexieder, T., (Ed.), Mechanisms of Cardiac Morphogenesis and Teratogenesis, vol. 5. Raven Press, New York, pp. 31–48.

Epstein, J.A., Li, J., Lang, D., Brown, C.B., Jin, F., Lu, M.M., Thomas, M., Liu, E., Wessels, A., Lo, C.W., 2000. Migration of cardiac neural crest cells in Splotch embryos. Development 127, 1869–1878.

Finkelmeier, B.A., Marolda, D., 2001. Aortic dissection. J. Cardiovasc Nurs. 15, 15–24.

Frank, D., Fotheringham, L., Brewer, J., Muglia, L., Tristani-Firouzi, M., Capecchi, M., Moon, A., 2002. An Fgf8 mouse mutant phenocopies human 22q11 deletion syndrome. Development 129, 4591–4603.

Garg, V., Yamagishi, C., Hu, T.H., Kathiriya, I.S., Yamagishi, H., Srivastava, D., 2001. Tbx1, a DiGeorge syndrome candidate gene, is regulated by Sonic hedgehog during pharyngeal arch development. Dev. Biol. 235, 62–73.

Hamburger, V., Hamilton, H.L., 1951. A series of normal stages in the development of the chick embryo. J. Morphol. 88, 49–92.

Jerome, L.A., Papaioannou, V.E., 2001. DiGeorge syndrome phenotype in mice mutant for the T-box gene, Tbx1. Nat. Genet. 27, 286–291.

Jiang, X., Rowitch, D.H., Soriano, P., McMahon, A.P., Sucov, H.M., 2000. Fate of the mammalian cardiac neural crest. Development 127, 1606–1616.

Kelly, R.G., Brown, N.A., Buckingham, M.E., 2001. The arterial pole of the mouse heart forms from Fgf10-expressing cells in pharyngeal mesoderm. Dev. Cell 1, 435–440.

Kirby, M.L., Gale, T.F., Stewart, D.E., 1983. Neural crest cells contribute to aorticopulmonary septation. Science 220, 1059–1061.

Kirby, M.L., Turnage, K.L., Hays, B.M., 1985. Characterization of conotruncal malformations following ablation of "cardiac" neural crest. Anat. Rec. 213, 87–93.

Kirby, M.L., Lawson, A., Stadt, H.A., Kumiski, D.H., Wallis, K.T., McCraney, E., Waldo, K.L., Li, Y.X., Schoenwolf, G.C., 2003. Hensen's node gives rise to the ventral midline of the foregut: implications for organizing head and heart development. Dev. Biol. 253, 175–188.

Kramer, T.C., 1942. The partitioning of the truncus and the formation of the membranous portion of the interventricular septum in the human heart. Am. J. Anat. 71, 343–370.

Le Lièvre, C.S., Le Douarin, N.M., 1975. Mesenchymal derivatives of the neural crest: analysis of chimaeric quail and chick embryos. J. Embryol. Exp. Morphol. 34, 125–154.

Li, J., Chen, F., Epstein, J.A., 2000. Neural crest expression of Cre recombinase directed by the proximal Pax3 promoter in transgenic mice. Genesis 26, 162–164.

Lough, J., Sugi, Y., 2000. Endoderm and heart development. Dev. Dyn. 217, 327–342.

Merscher, S., Funke, B., Epstein, J.A., Heyer, J., Puech, A., Lu, M.-M., Xavier, R.J., Demay, M.B., Russell, R.G., Factor, S., et al., 2001. TBX1 is responsible for cardiovascular defects in velo-cardio-facial/DiGeorge syndrome. Cell 104, 619–629.

Miyagawa-Tomita, S., Waldo, K., Tomita, H., Kirby, M.L., 1991. Temporospatial study of the migration and distribution of cardiac neural crest in quail–chick chimeras. Am. J. Anat. 192, 79–88.

Mjaatvedt, C.H., Nakaoka, T., Moreno-Rodriguez, R., Norris, R.A., Kern, M.J., Eisenberg, C.A., Turner, D., Markwald, R.R., 2001. The outflow tract of the heart is recruited from a novel heart-forming field. Dev. Biol. 238, 97–109.

Patten, F.M., 1953. In: Gould, S.E. (Ed.), Pathology of the Heart and Blood Vessels, Charles C. Thomas, Springfield, IL.

Thompson, R.P., Fitzharris, T.P., 1979. Morphogenesis of the truncus arteriosus of the chick embryo heart: the formation and migration of mesenchymal tissue. Am. J. Anat. 154, 545–556.

Thompson, R.P., Fitzharris, T.P., 1985. Division of cardiac outflow. In: Ferrans, V., Rosenquist, G., Weinstein, C. (Eds.), Cardiac Morphogenesis, Elsevier Science Publishing Co., Inc., Amsterdam.

Van Mierop, L.H.S., 1979. Morphological development of the heart. In: Berne, R.M., Sperelakis, N., Geiger, S.R. (Eds.), Handbook of Physiology—The Cardiovascular System, Waverly Press, Baltimore, pp. 1–28.

Vitelli, F., Morishima, M., Taddei, I., Lindsay, E.A., Baldini, A., 2002. Tbx1 mutation causes multiple cardiovascular defects and disrupts neural crest and cranial nerve migratory pathways. Hum. Mol. Genet. 11, 915–922.

Waldo, K.L., Kumiski, D., Kirby, M.L., 1994. Association of the cardiac neural crest with development of the coronary arteries in the chick embryo. Anat. Rec. 239, 315–331.

Waldo, K.L., Kumiski, D., Kirby, M.L., 1996. Cardiac neural crest is essential for the persistence rather than the formation of an arch artery. Dev. Dyn. 205, 281–292.

Waldo, K., Miyagawa-Tomita, S., Kumiski, D., Kirby, M.L., 1998. Cardiac neural crest cells provide new insight into septation of the cardiac outflow tract: aortic sac to ventricular septal closure. Dev. Biol. 196, 129–144.

Waldo, K.L., Lo, C.W., Kirby, M.L., 1999. Connexin 43 expression reflects neural crest patterns during cardiovascular development. Dev. Biol. 208, 307–323.

Waldo, K.L., Kumiski, D.H., Wallis, K.T., Stadt, H.A., Hutson, M.R., Platt, D.H., Kirby, M.L., 2001. Conotruncal myocardium arises from a secondary heart field. Development 128, 3179–3188.

Waldo, K.L., Hutson, M.R., Stadt, H.A., Zdanowicz, M., Zdanowicz, J., Kirby, M.L., 2005. Cardiac neural crest is necessary for normal addition of the myocardium to the arterial pole from the secondary heart field. Dev. Biol. 281, 66–77.

Xu, H., Morishima, M., Wylie, J.N., Schwartz, R.J, Bruneau, B.G., Linsay, E.A., Baldini, A., 2004. Tbx1 has a dual role in the morphogenesis of the cardiac outflow tract. Development 131, 3217–3227.

Ya, J., Schilham, M.W., Clevers, H., Moorman, A.F.M., Lamers, W.H., 1997. Animal models of congenital defects in the ventriculoarterial connection of the heart. J. Mol. Med. 75, 551–566.

Yablonka-Reuveni, Z., Christ, B., Benson, J.M., 1998. Transitions in cell organization and in expression of contractile and extracellular matrix proteins during development of chicken aortic smooth muscle: evidence for a complex spatial and temporal differentiation program. Anat. Embryol. 197, 421–437.

Yagi, H., Furutani, Y., Hamada, H., Sasaki, T., Asakawa, S., Minoshima, S., Ichida, F., Joo, K., Kimura, M., Imamura, S., et al., 2003. Role of TBX1 in human del22q11.2 syndrome. Lancet 362, 1366–1373.

Yamauchi, Y., Abe, K., Mantani, A., Hitoshi, Y., Suzuki, M., Osuzu, F., Kuratani, S., Yamamura, K., 1999. A novel transgenic technique that allows specific marking of the neural crest cell lineage in mice. Dev. Biol. 212, 191–203.

Yelbuz, T.M., Waldo, K.L., Kumiski, D.H., Stadt, H.A., Wolfe, R.R., Leatherbury, L., Kirby, M.L., 2002. Shortened outflow tract leads to altered cardiac looping after neural crest ablation. Circ. Res. 106, 504–510.